Enhancement of Coating Uniformity With Secondary Gas Atomization in Wire Arc Spray

X.Wang; J.Heberlein; E.Pfender; W.Gerberich

ERC for Plasma-Aided Manufacturing
University of Minnesota, Mpls, MN 55455

ABSTRACT

Traditionally, only primary gas is used as the atomizing gas in the wire arc spray coating process. In this case, the coating microstructures and properties vary from center to edge because of the wide droplet trajectory distribution. We have conducted experiments in which a secondary shroud gas is used to reduce the divergence of the droplet trajectories. In this study, stainless steel is sprayed onto aluminum substrates with (1) only primary gas atomization and (2) both primary and secondary gas atomization. Pitot tube measurements of the atomizing cold gas velocity at the nozzle exit show that the gas velocity in case (2) is higher than that in case (1). Trajectories of the droplets are observed with a laser strobe high speed video camera. High speed images and spray pattern observations show that secondary gas injection leads to more focused droplet trajectories. Simultaneous arc voltage fluctuation records indicate that the secondary gas does not affect the waveform and frequency of arc fluctuations. Particles are collected by spraying into an ice sheet and particle size distributions are measured using image analysis. Coating porosities are measured using scanning electron microscopy combined with image analysis and adhesion strength is measured with an Instron tensile machine using the ASTM C-733 method. The results show that smaller droplets, lower porosity and higher adhesion strength are obtained by using a secondary gas injection.

INTRODUCTION

Arc spraying is used widely to coat engineering structures in order to protect them against corrosion and wear [1,2]. To achieve these objectives, coatings with minimal porosity and maximum strength are required [3]. However, the velocities of the particles are subject to certain limitations, so the coating produced with conventional primary gas atomization has relatively high porosity and relatively low bonding strength. Secondary gas atomization spraying is a newly developed approach in order to achieve uniform particle size distributions, more focused spray pattern, higher particle velocities and to improve the coating properties. A modified nozzle with secondary gas injection as shown in Fig.1 has been developed to optimize atomization

and enhance particle velocities. A primary axial air stream impinges upon the wire tips to cause the molten metal to be carried axially away from the area of the wire intersection, and a secondary air stream forms a conical sheath around the axial air stream. The primary gas stream and the secondary gas stream emerge from the nozzle as coaxial gas streams thus tending to protect the droplets from entrained air and to concentrate the flow pattern of the droplets.

EXPERIMENTAL PROCEDURES

Sample Preparation and Operating Conditions. Before spraying, the aluminum substrates have been treated by grit blasting, acetone degreasing and ultrasonic cleaning. Stainless steel has been sprayed under the following conditions: primary atomizing gas pressure: 60psi ; secondary gas pressure: 30psi; arc voltage: 30V; arc current: 150A; stand-off distance: 15cm.

Sample Analysis.

Scanning Electron Microscopy. Micrographs of polished coating cross-sections and particle morphology have been investigated using scanning electron microscopy.

Digital Image Analysis. Image analysis has been used to determine the porosity of polished coating cross-sections. The analysis uses differences in grey levels to distinguish the different features of the coating microstructure. Features such as porosity have been detected through their respective grey scale ranges, and pore sizes have been measured. In order to obtain average results, the porosity measurements have been performed for twelve different locations randomly distributed over the coating cross-sections.

Wavelength Dispersive Spectroscopy . WDS is a non-destructive technique with a sensitive depth resolution suitable for element analysis of materials. The sample surface has been etched to a depth of 300 Å by argon ion beam sputtering which eliminates surface contamination. The atomic concentrations have been calculated from the intensity of the peaks based on relative sensitivity calibration.

Adhesive Bond Strength Test:. According to ASTM C633-79 standard, a pull-off tensile test determines the degree of adhesion of a coating to a substrate in tension normal to the surface. Tests have been carried out by using an Instron machine with a cross-head speed of 0.03 inch/minute.

Measurement of Diameter of Spray Pattern. The approach for measurement of diameter of spray pattern is shown in Fig. 1. The molten droplets are deposited onto a big plate which is 15cm far from the spray gun head. The diameter of the deposits measured is defined as diameter of the spray pattern.

Gas Velocity Measurement. A Pitot tube is used to measure the atomizing cold gas velocity at the nozzle exit.

Process Diagnostics. The experimental set-up for process diagnostics is shown in Fig. 2. Images of the luminous arc, of the wire electrodes, and of the droplet formation have been recorded with a laser strobe high speed camera. The corresponding arc voltage between the consumable electrodes has been simultaneously recorded with an oscilloscope. Laser A (Fig. 2) is used to illuminate the wire tips which are photographed with the high speed CCD camera with 100 ns shutter speed. The light beam reflected by a mirror from laser B is transformed into an electrical signal by a photo-detector, which triggers the oscilloscope. The rotating timing wheel (Fig. 2) with two shutter windows is adjusted by a speed controller and allows simultaneous recording of the high speed images through one window and triggering of the oscilloscope by passing the second laser beam through the second window.

Results and Discussions

Arc Characteristics. During the spraying process, the wire melting rate and the wire feed rate are not perfectly matched, forcing a more or less periodic variation of the arc length. The large variation in droplet size is due to this periodic variation in arc length. The relatively long time voltage trace in Fig. 3 shows these almost periodic voltage fluctuations for the primary gas atomization and primary/secondary gas atomization. These voltage fluctuations confirm the previously observed arc gap fluctuations with a period of approximately 2 ms. Fourier transformation analysis of the voltage trace indicates that the frequency of the fluctuation is approximately 500 Hz. It is apparent that these arc fluctuations occur with both primary gas atomization and primary/secondary gas atomization at the same frequency, indicating that the additional secondary atomizing gas does not change the arcing behavior.

Gas Velocity, Spray Trajectory and Spray Pattern. The gas velocity results show that the gas velocity (600 m/s) at nozzle exit in the case of primary/secondary air atomization is higher than that (560 m/s) in the case of primary air atomization. Fig. 4 shows high speed images of particle flight trajectories. It appears that secondary gas addition focuses the particle flight trajectories. This is corroborated with results of diameter of spray pattern measurements. The diameter of the spray pattern in the case of primary/secondary gas atomization (14cm) is smaller than that in the case of primary gas atomization (24cm).

Particle Size Distributions. Droplet size has been determined by spraying into ice and observing the resulting solidified particles with a scanning electron microscope. Fig. 5 shows the morphology of particles sprayed under two conditions: (a) primary air atomization; (b) primary/secondary air atomization. The particle size is smaller in the case of primary/secondary air atomization. This is due to the fact that the secondary gas leads to more efficient atomization of the molten wire tips breaking some larger droplets from the anode into smaller particles. Image analysis is used to analyze size distribution of particles sprayed under the two conditions. In both cases, the size distribution shows a dual mode. The lower peak is probably due to the smaller particles from the cathode whose temperature tends to be locally higher, while the second peak is due to the larger particles from the anode which reveals bulk melting. Using the secondary air flow, a narrower particle size distribution is obtained which is important for producing uniform coating microstructures.

Coating Microstructure. The coating structure is determined by the particle velocity and the particle temperature at the instant of impact on the substrate. Completely molten particles impinging on the substrate spread out radially in the form of thin discs. In reality, however, the deposit is not uniform in thickness and the periphery of the flattened particle is not circular. Fig. 6 shows the surface morphology of stainless steel coatings prepared with the primary gas atomization and primary/secondary gas atomization. It is obvious that the flattening behavior is different for the two cases. The molten particles sprayed with the primary/secondary gas atomization spread out to a much greater extent than those sprayed with only the primary gas atomization. They also show a higher degree of deformation, and there are less unmolten droplets at the edges of the flattened particles. Fig. 7 shows cross-sectional views of coatings sprayed with the primary gas atomization and with the primary/secondary gas atomization illustrating that the coatings prepared with the primary/secondary gas atomization have lower porosity than those produced with the primary gas atomization. Also, In the case of primary/secondary gas atomization, the porosity over the entire cross-section does not change appreciably (7% at the edge, 6% in the center), while in the case of primary gas atomization, the porosity varies

significantly from the edge (21%) to the center (12%). These observations are readily explained by the higher velocity of the atomizing gas stream, more focused spray jet and more uniform particle size distribution obtained with secondary gas atomization. In wire arc spraying, the particle has its highest temperature in front of the wire electrode, and a higher atomizing gas velocity will lead to a higher acceleration of the particle. The consequence is not only a higher impact velocity, but also a higher particle temperature at impact because of the shorter flight time and less cooling by entrained air. The higher temperatures result in lower viscosities and better wettabilities, yielding better conformal coatings in the case of adding the secondary atomizing gas.

Bond Strength. A significant criterion for the quality of thermally-sprayed films is their adhesion to the substrate. The coating is built up particle by particle [4,5]. Molten particles undergo severe deformation and rapid solidification when they impinge on the substrate. To achieve high bonding strength between film and substrate, the particles must be in a fully molten state and have sufficient velocities to be able to spread out and flow into the contours and crevices of the roughened substrate. The results of adhesion tests indicate that the bond strength of the stainless steel coating sprayed with the primary/secondary gas atomization (37 MPa) is higher than that sprayed with only primary gas atomization (26 Mpa). In general, higher adhesive bond strength is due to the higher velocity of the molten particles when impacting on the substrate in the case of using the secondary gas atomization.

Oxide Content. The amount of oxide depends on both the amount of oxygen present in the spraying jet and the total surface area of the particles in the jet. The amount of oxide in the primary/secondary air atomizing sprayed coating (29%) is higher than that of the only primary air atomizing sprayed coating (20%). During spraying, the effect of atomizing air and the entrainment of the surrounding air into the spray stream cause significant in-flight oxidation of the molten metal particles [4,5]. Secondary air atomization leads to higher gas stream velocities, which in turn breaks up the molten particles more finely. The smaller particles react more readily with oxygen than the larger ones, because of their greater specific surface area. Thus coatings sprayed under primary/secondary air atomization tend to show higher oxide content. If the oxide content needs to be kept low, non-reactive gases have to be used for atomization, and the secondary gas can in this case provide a shroud.

CONCLUSION

Compared to only primary gas atomization in wire-arc-spraying, the adding of secondary gas is capable of atomizing the particles to smaller sizes with more uniform distribution and accelerating them to higher velocities. Thus, the porosity of coatings prepared with primary/secondary gas atomization are decreased. Also the microstructure of coatings is much more uniform from center to edge. Adhesive bond strength of coatings sprayed with primary/secondary gas atomization is increased.

ACKNOWLEDGMENTS

This work has been supported by NSF through the ERC for Plasma-Aided Manufacturing grant ECD-87-21545. The government has certain rights in this material.

REFERENCES

[1] H.-D.Steffens, Z.Babiak and M.Wewel, "Recent developments in arc spraying", IEEE Transactions on Plasma Science, 18/6,(1990).

[2] M.L.Thorpe, "Thermal spray applications grow" Adv. Mat. Proc., VOL. 134, (1988).

[3] David R.Marantz, Daniel R. Marantz, "State of the art arc spray technology", Thermal Spray Research and Applications, Proceedings of the Third National Thermal Spray Conference, p 113, Long Beach, CA,20-25, May, (1990).

[4] E.Pfender, "Fundamental studies associated with the plasma spray process", Surface and Coating Technology, 34, p. 8,(1988).

[5] E.Pfender, Thin Solid Films, P. 228-241, 238, (1994)

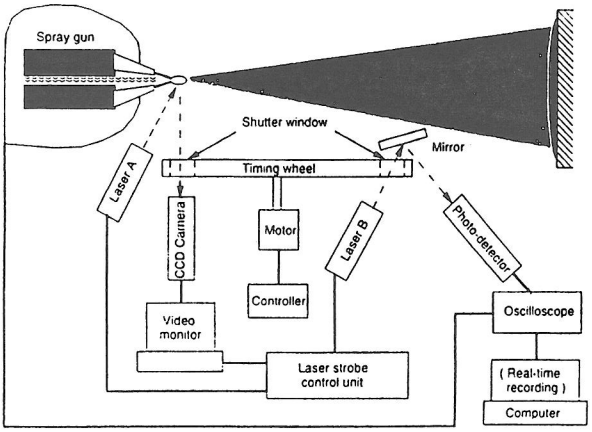

Fig. 2 - Process diagnostic setup

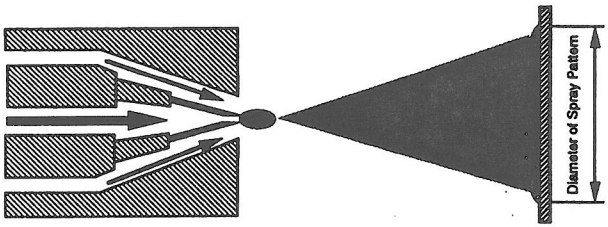

Fig. 1 - Cross-sectional schematic of nozzle with secondary gas injection

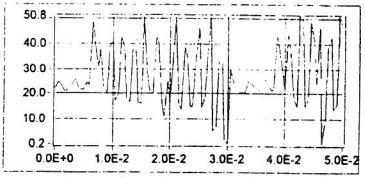

Primary gas atomization

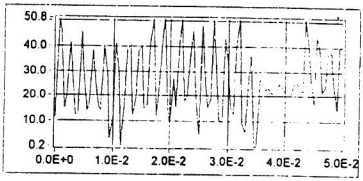

Primary/secondary gas atomization

Fig. 3 - Voltage traces of arc fluctuation

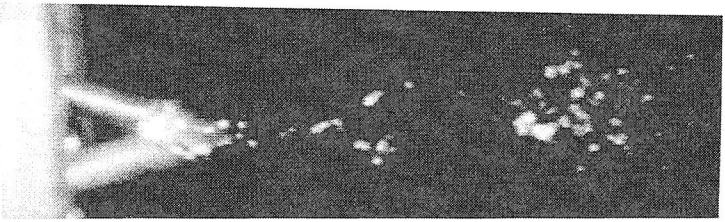

Primary gas atomization

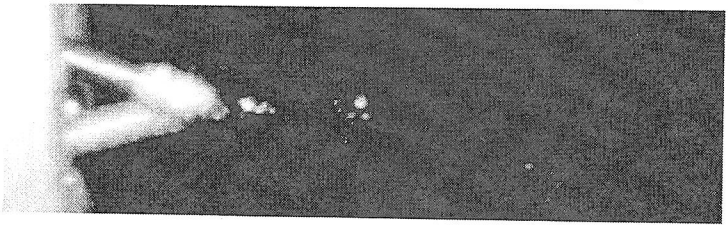

Primary/secondary gas atomization

Fig. 4 - High speed images of particle flight trajectory

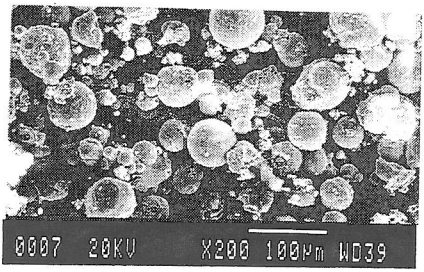

Primary gas atomization

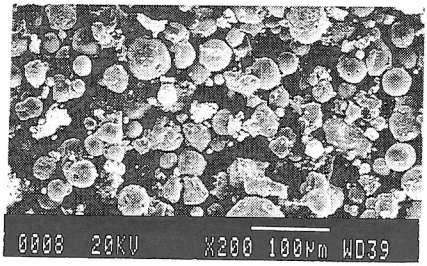

Primary/secondary gas atomization

Fig. 5 - Scanning electron micrograph of particles

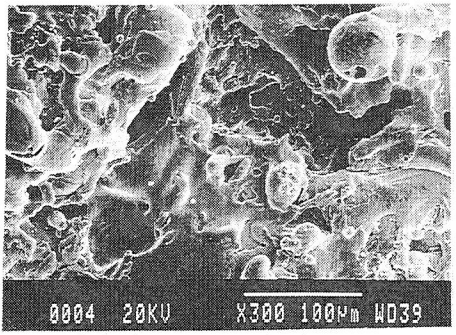

Primary gas atomization

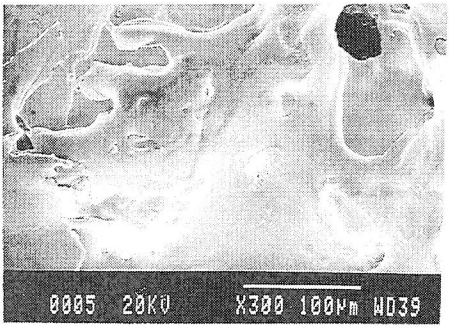

Primary/secondary gas atomization

Fig. 6 - Surface morphology of coatings

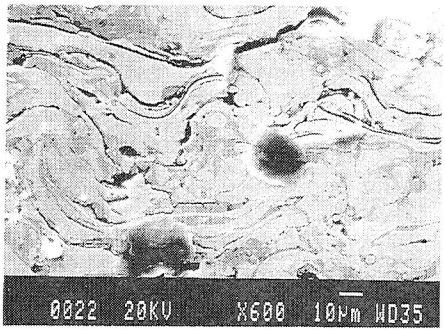

center

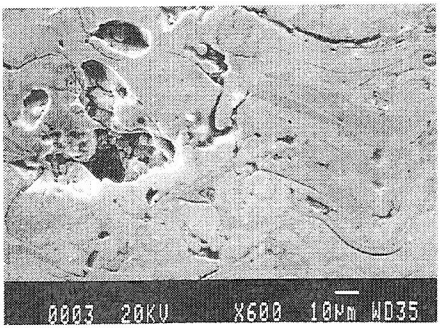

edge

Primary gas atomization

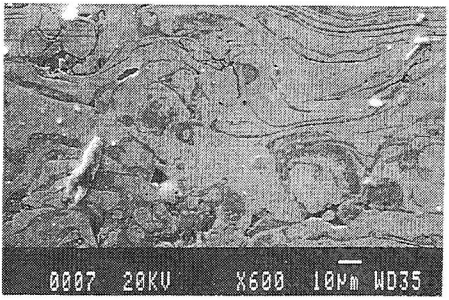

center

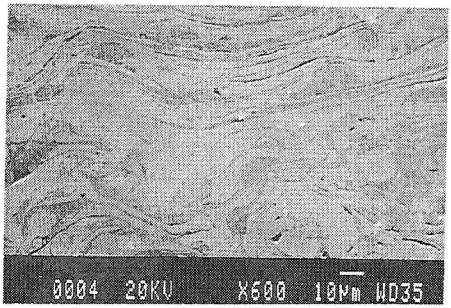

edge

Primary/secondary gas atomization

Fig. 7 - SEM of cross-section of coatings